ANISOTROPIC MECHANICAL PROPERTIES IN A BIG-SIZED Ti-6Al-4V PLATE FABRICATED BY ELECTRON BEAM MELTING

Pan Wang[1], Mui Ling Sharon Nai[1], Xipeng Tan[2], Wai Jack Sin[1], Shu Beng Tor[2], Jun Wei[1]

[1]Singapore Institute of Manufacturing Technology, 71 Nanyang Drive, 638075, Singapore
[2]Singapore Centre for 3D Printing, School of Mechanical & Aerospace Engineering, Nanyang Technological University, HW1-01-05, 2A Nanyang Link, 637372 Singapore

Keywords: Additive manufacturing; Electron beam melting; Titanium alloy; Anisotropy; Mechanical properties

Abstract

In this study, in order to realize the application of the electron beam melting (EBM) technology for the printing of large components, the microstructure and mechanical properties of a big-sized Ti-6Al-4V plate (6 mm×180 mm×372 mm) additively manufactured by EBM were investigated. The paper focused on the graded microstructure and anisotropic mechanical properties by using x-ray diffraction, optical microscope, scanning electron microscope, microhardness and tensile test. A gradual change in microstructure with an increase in build height was observed. The formation of a graded microstructure was observed and discussed based on the thermal history experienced during printing. The mechanical properties were influenced accordingly by the graded microstructure. Moreover, the specimens which were printed parallel and perpendicular to the printing directions exhibited high elongation of ~18% and ~14%, respectively. The anisotropy in ductility was also observed and discussed according to the columnar prior β structure and grain boundary α phases present.

Introduction

Additive manufacturing (AM) technologies shorten the design to product time and reduce the process steps involved [1-3] thus overcoming some limitations of the traditional manufacturing methods like casting [4], forging [5, 6] and rolling [7]. In particular, AM technologies have exhibited promising applications in high value added industries [1, 8, 9]. Electron beam melting (EBM) is one of the layer-by-layer AM techniques, which has the capability of producing near-net shaped parts with complex geometries. Furthermore, due to its vacuum controlled process and high energy electron beam, it can be used to process high melting point and reactive metallic materials. Therefore, it is suitable for fabricating Ti alloy parts for the aerospace and biomedical applications [10, 11].

Layer-by-layer fusion step in EBM introduces rapid thermal cycles, which results in a different microstructure as compared to their cast or wrought counterparts. Moreover, the previous layers experience a thermal history during printing and this further introduces a different thermal history for each subsequent layer. In order to ensure the use of these printed parts in structural applications, their mechanical properties must be characterized. Therefore, many researchers have focused on understanding the microstructure and mechanical properties of Co-Cr-based alloys [12], Ti alloys [11, 13, 14] and Ni-based alloys [15] fabricated by EBM technology. Although these results exhibited excellent mechanical properties, the previous

investigations only focused on small build samples and/or parts with short build heights. However, for industry applications, in particular, aerospace applications, a big-sized part with complex shape is of actual industrial need. Recently, graded microstructure and mechanical properties were reported by Tan *et al.* in a 10 mm×100 mm× 30 mm block [16]. However, there is still lack of understanding with regards to the microstructure and mechanical properties of big-sized parts. Moreover, anisotropic tensile behavior of directed energy deposition additive manufactured Ti-6Al-4V was reported [17]. It is suggested that the presence of grain boundary α phase plays a critical role on the anisotropic ductility. Therefore, it is reasonable to predict that anisotropic mechanical properties may also appear in the EBM-built parts. Accordingly, in the present study, the effects of build height on the microstructure and mechanical properties of a big-sized plate were investigated. The anisotropic mechanical properties were also discussed.

Experimental procedures

An Arcam A2X EBM system with a build envelope of 200mm×200mm×380mm was used (software version 3.2, accelerating voltage 60,000 V, layer thickness 50 μm, Arcam AB standard build theme for Ti-6Al-4V alloy) to print four plates (6 mm×180 mm×372 mm in thickness, length and height, respectively) centered on a 210 mm×210 mm stainless steel start plate. Fig. 1 (a) shows an as-built plate. The pre-alloyed Ti–6Al–4V (Grade 5) virgin powder with a nominal composition of Ti-6Al-4V-0.03C-0.1Fe-0.15O-0.01N-0.003H supplied by Arcam AB, was used in the present study. After ~1 hour vacuum, the 10 mm thick start plate was heated when both a chamber pressure and an electron beam column pressure reached to below 5×10^{-4} mbar and 5×10^{-6} mbar, respectively. The four big-sized Ti-6Al-4V plates were directly built on the preheated start plate once the bottom temperature that was measured by a thermal couple placed beneath the start plate reached 730 ℃. High-purity helium was applied to regulate a vacuum of $\sim2\times10^{-3}$ mbar during the building process.

In order to examine the microstructure and mechanical properties of the printed plate, tensile specimens were wire-cut from the plate in two orientations (parallel and perpendicular to build direction). In each orientation, they were divided into three groups of specimens that were taken from the bottom, middle and top sections, respectively (Fig. 1 b). The dimensions of tensile specimens were illustrated in Fig. 1 (c). The surface of all the tensile specimens was smoothened by plunge grinding. The tensile test was conducted at room temperature in air, at an initial strain rate of 3.3×10^{-4} s^{-1}, using the Instron 4505 universal tensile testing machine with a load cell capability of 100 kN. In addition, an extensometer was applied to measure the strain. Microhardness tests were conducted on the polished specimens by using a micro hardness tester (Mitutoyo MVK-G350AT) with a load of 300 gf and a dwell time of 15 seconds. The specimens for microhardness tests were cut at a build height of ~13 mm (Fig. 1 b).

Phase identification was carried out using the X-ray diffraction (XRD), at room temperature with Cu K_α radiation operated at 40 kV and 40 mA. Microstructural observation was conducted using an optical microscope (OM) after etching by the Kroll's reagent. Scanning electron microscopy (SEM) was also used for microstructural analysis.

Results

Some small spherical pores (Fig. 2 a) with an average diameter of ~12 μm and irregular pores (Fig. 2 b) were occasionally observed. This is a common phenomenon in AM Ti-6Al-4Vparts

[17-19] due to the eargon during the production of gas atomized Ti-6Al-4V powder and the lack of fusion during layerwise melting [10, 18]. It is also worth noting that any spherical or irregular pores are supposed to be detrimental to fatigue properties while those small spherical pores in Fig. 2a may not significantly affect the tensile properties.

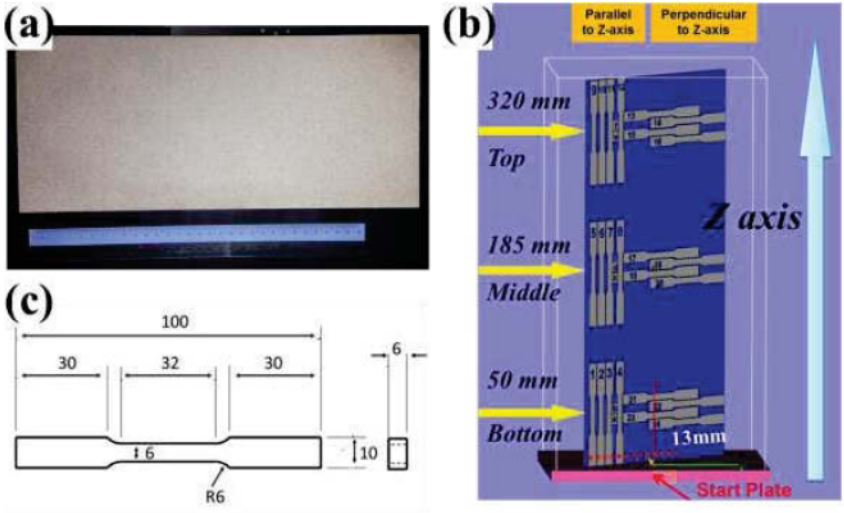

Fig. 1 (a) Picture of plate fabricated by EBM, (b) schematic illustration of locations of tensile specimens and microhardness specimens cut from plate, and (c) dimensions of tensile specimens in mm. The tensile specimens was divided into two groups, parallel to Z axis and perpendicular to Z axis. The microhardness was measured along the red round dot lines, which was ~13 mm high. It is noted that the microhardness specimens were cut from another plate as continuous microhardness values across the plate (from the left edge) were desired.

The microstructures at the bottom (Fig. 3 a and d), middle (Fig. 3 b and e) and top (Fig. 3 c and f) regions in the Ti-6Al-4V plate were shown in Fig. 3. Regardless of the build height (Fig. 3 a-c), columnar grain structures were clearly observed in all the three specimens. The columnar prior β grain is a typical feature of EBM-built Ti-6Al-4V part because of the high thermal gradient along Z axis, which has been reported eleswhere [13, 16]. The microstructure contained grain boundary α and transformed α + β microstructure within the columnar prior β grains. Only ~8 layers were shown in Fig. 3 (a) because the build layer thickness is 50 μm. However, the columnar prior β grains obviously grow across many layers, which differs from that manufactured by selective laser melting and laser aided additive manufacturing.

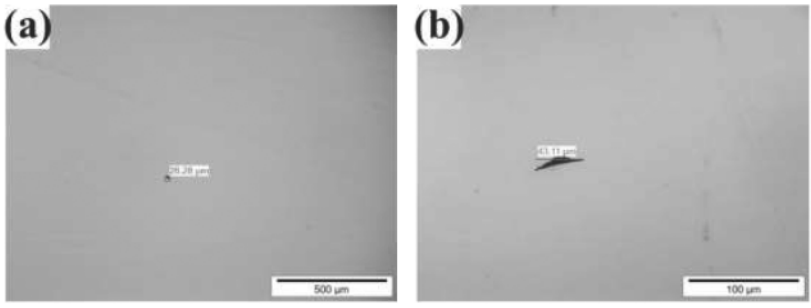

Fig. 2 Optical microscopy images of (a) the typical pore and (b) lack of fusion pore observed in Ti-6Al-4V plate fabricated by EBM.

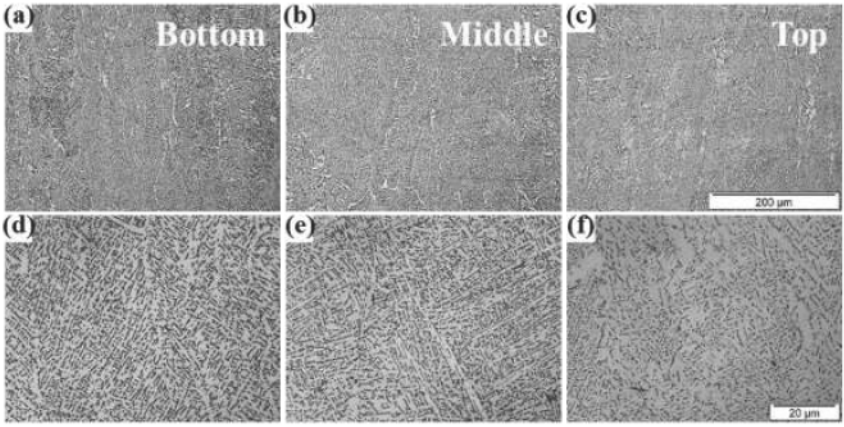

Fig. 3 Optical microscopy images of (a, d) bottom, (b, e) middle (c, f) top regions in the Ti-6Al-4V plate fabricated by EBM. (a-c) show columnar structure by using low magnification and (d-f) show α + β microstructure by using high magnification.

Fig. 3 (d-f) show the high magnification optical micrographs from the bottom region to the top region. Only α phase and β phase were observed, regardless of the build height. Because phase constitution and their distribution strongly influenced the mechanical properties [4, 13, 20] and α′ martensitic phase may exist in the EBM-built Ti-6Al-4V [11, 21], XRD measurements [22] and SEM analysis were carried out. It is confirmed that only α phase and a relatively small fraction of β phase exist in the present plate. However, the α lath width increased with an increase in build height. In particular, the α lath width was observed to increase from the middle region (Fig. 3. e) to the top region (Fig. 3 f). The graded microstructure was also observed in Co-Cr alloy fabricated by EBM [12]. This is caused by the effect of different thermal histories on different build heights. The increase of α lath width is attributed to the slower cooling rate in the top region. Since the bottom build directly connects to the stainless steel start plate, the heat

inside the bottom region is easily transferred to the start plate and then spread out. However, with the increase in build height, it becomes challenging to transfer the heat to the bottom region as quickly as compared to the stainless steel start plate due to the low thermal conductivity of Ti-6Al-4V solid, which is even worse for the case of Ti-6Al-4V powder [23]. A long exposure at higher temperatures on the top region resulted in the coarser α phase lath widths.

Fig. 4 shows the microhardness values measured from left edge to center at a build height of ~13 mm. All the measured values were around 340 HV and no significant difference was observed at the same build height. These results indicated that the tensile specimens wire-cut from the plate (Fig. 1 b) will yield the same tensile properties because those designated layers underwent the same thermal history in the present study.

Fig. 5 shows the Young's modulus at different build heights and orientations. It was observed that their Young's modulus values in the present study were almost constant, which is consistent with the finding of the previous report [10].

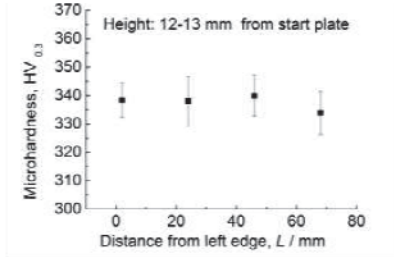

Fig. 4 Trend of microhardness values across the EBM printed Ti-6Al-4V plate (from the left edge), at a height of ~ 13mm from the start plate.

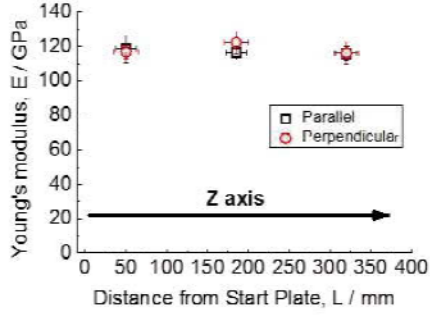

Fig. 5 Trend of Young's modulus values of the EBM printed Ti-6Al-4V plate (from the base of the start plate).

Fig. 6 shows the stress-strain tensile curves at room temperature. Similar to the commercial wrought Ti-6Al-4V, only a weak work hardening phenomenon was observed. Both the yield

strength and ultimate tensile strength were found to be dependent on the build height and orientation. These strength values were comparable to the results reported by S.S. Al-Bermani *et al.* [13] and that of the wrought Ti-6Al-4V according to ASTM 1472-14 [24]. Moreover, the yield strength and ultimate tensile strength were observed to decrease with an increase in build height. This is attributed to the finer α + β microstructure. It has been reported that the yield strength decreased with the increase of α lath width in Ti-6Al-4V alloys [13].

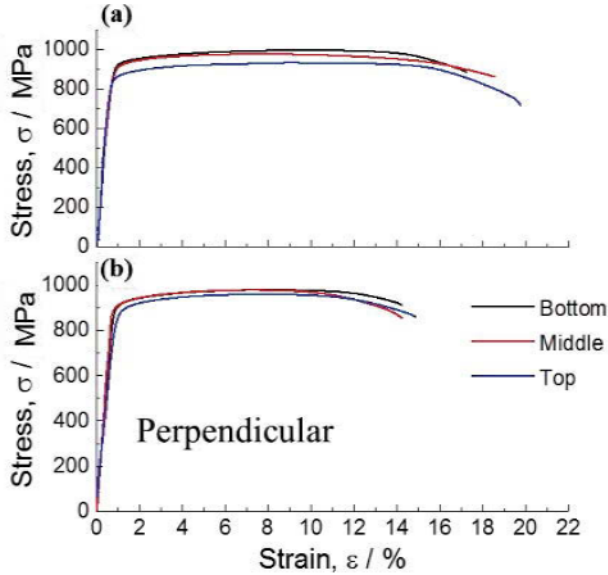

Fig. 6 Stress-strain curve of (a) parallel and (b) perpendicular to Z-axis specimens cut from Ti-6Al-4V plate fabricated by EBM.

On the other hand, more than 14% deformation strains were obtained in all the EBM printed specimens, regardless of their build height and orientation. These values were higher than that of the wrought form (ASTM 1472-14, 10%) [24]. It should be noted that the plastic strain in parallel orientation (~18%) was higher than that of perpendicular orientation (~14%). It is suggested that the anisotropy in ductility is mainly attributed to the appearance of the grain boundary α phase. The grain boundary α phase (Fig. 3 a-c) provides a preferential path for damage accumulation along the grain boundary. When a load is applied to the orientation perpendicular to the prior β grain boundary, a tensile opening mode is subjected to accelerated damage [17]. Therefore, a low plastic strain was observed in the perpendicular orientation (Fig. 6).

Conclusions

The graded microstructure as well as the anisotropic mechanical properties of a big-sized Ti-6Al-4V plate (6mm×180mm×372mm) were investigated. The following conclusions can be drawn.

(1) Columnar grain structure containing grain boundary α phase and transformed α + β microstructure within the prior β grain were observed, regardless of the build height.
(2) Only α phase and a relatively small fraction of β phase were detected in the microstructure of the as-built Ti-6Al-4V specimens. The α phase lath width increased with an increase in build height.
(3) With the increase in build height, the yield strength and ultimate tensile strength of the specimens were found to decrease. This is attributed to the increase of α lath width due to the different thermal histories along the build height.
(4) Anistropic mechanical properties was observed because of the presence of grain boundary α. A low deformation strain (~14%) was obtained in the perpendicular orientation and a high deformation strain (~18%) was obtained in the parallel orientation.
(5) The yield strengh and ultimate tensile strength of all the examined specimens were comparable to that of the wrought material and their elongations were even higher (ASTM 1472-14).

References

[1] Zhai Y, Lados DA, LaGoy JL. Additive manufacturing: making imagination the major limitation. JOM. 2014;66:808-16.
[2] Gong X, Anderson T, Chou K. Review on powder-based electron beam additive manufacturing technology. Manufacturing Review. 2014;1:2.
[3] Frazier WE. Metal additive manufacturing: A review. Journal of Materials Engineering and Performance. 2014;23:1917-28.
[4] Wang P, Feng Y, Liu F, Wu L, Guan S. Microstructure and mechanical properties of Ti–Zr–Cr biomedical alloys. Materials Science and Engineering: C. 2015;51:148-52.
[5] Guan S, Wu L, Wang P. Hot forgeability and die-forging forming of semi-continuously cast AZ70 magnesium alloy. Materials Science and Engineering: A. 2009;499:187-91.
[6] Wang P, Zhu S, Wang L, Wu L, Guan S. A two-step superplastic forging forming of semi-continuously cast AZ70 magnesium alloy. Journal of Magnesium and Alloys. 2015;3:70-5.
[7] Yi C, Guan S, Lu G, Zhao H, Wang P. Influence of annealing process on microstructure and properties of twin-roll cast 5052 aluminium alloy [J]. Transactions of Materials and Heat Treatment. 2011;4:013.
[8] Greenemeier L. To Print the Impossible. Scientific American. 2013;308:44-7.
[9] Lipson H, Kurman M. Fabricated: The new world of 3D printing: John Wiley & Sons; 2013.
[10] Murr L, Esquivel E, Quinones S, Gaytan S, Lopez M, Martinez E, et al. Microstructures and mechanical properties of electron beam-rapid manufactured Ti–6Al–4V biomedical prototypes compared to wrought Ti–6Al–4V. Materials Characterization. 2009;60:96-105.
[11] Ikeo N, Ishimoto T, Nakano T. Novel powder/solid composites possessing low Young's modulus and tunable energy absorption capacity, fabricated by electron beam melting, for biomedical applications. Journal of Alloys and Compounds. 2015;639:336-40.
[12] Sun S-H, Koizumi Y, Kurosu S, Li Y-P, Chiba A. Phase and grain size inhomogeneity and their influences on creep behavior of Co–Cr–Mo alloy additive manufactured by electron beam melting. Acta Materialia. 2015;86:305-18.
[13] Al-Bermani S, Blackmore M, Zhang W, Todd I. The origin of microstructural diversity, texture, and mechanical properties in electron beam melted Ti-6Al-4V. Metallurgical and Materials Transactions A. 2010;41:3422-34.

[14] Kok Y, Tan X, Tor SB, Chua CK. Fabrication and microstructural characterisation of additive manufactured Ti-6Al-4V parts by electron beam melting. Virtual and Physical Prototyping. 2015;10:13-21.
[15] Prabhakar P, Sames W, Dehoff R, Babu S. Computational modeling of residual stress formation during the electron beam melting process for Inconel 718. Additive Manufacturing. 2015.
[16] Tan X, Kok Y, Tan YJ, Descoins M, Mangelinck D, Tor SB, et al. Graded microstructure and mechanical properties of additive manufactured Ti–6Al–4V via electron beam melting. Acta Materialia. 2015;97:1-16.
[17] Carroll BE, Palmer TA, Beese AM. Anisotropic tensile behavior of Ti–6Al–4V components fabricated with directed energy deposition additive manufacturing. Acta Materialia. 2015;87:309-20.
[18] Tammas-Williams S, Zhao H, Léonard F, Derguti F, Todd I, Prangnell P. XCT analysis of the influence of melt strategies on defect population in Ti–6Al–4V components manufactured by Selective Electron Beam Melting. Materials Characterization. 2015;102:47-61.
[19] Mok SH, Bi G, Folkes J, Pashby I. Deposition of Ti-6Al-4V using a high power diode laser and wire, Part I: Investigation on the process characteristics. Surf Coat Technol. 2008;202:3933-9.
[20] Pan W, Todai M, Nakano T. β-Phase Instability in Binary Ti-xNb Biomaterial Single Crystals. Materials Transactions. 2013;54:156-60.
[21] Tan X, Kok Y, Tan YJ, Vastola G, Pei QX, Zhang G, et al. An experimental and simulation study on build thickness dependent microstructure for electron beam melted Ti–6Al–4V. Journal of Alloys and Compounds. 2015;646:303-9.
[22] Wang P, Nai MLS, Sin WJ, Wei J. Effect of building height on microstructure and mechanical properties of big-sized Ti-6Al-4V plate fabricated by electron beam melting. Advanced Materials Research: Trans Tech Publ; 2015.
[23] Lütjering G, Williams JC. Titanium: Springer; 2003.
[24] International A. Standard Specification for Wrought Titanium-6Aluminum-4Vanadium Alloy for Surgical Implant Applications (UNS R56400). West Conshohocken, PA: ASTM International; 2014.